Astronomy & Astrophysics manuscript no. SamCir˙astroph
November 5, 2008
© ESO 2008

arXiv:0811.0698v1 [astro-ph] 5 Nov 2008

MOND vs. Newtonian dynamics in early-type galaxies

The case of NGC 4649 (M60)

S. Samurović[1] and M.M. Ćirković[1]

[1]Astronomical Observatory, Volgina 7, 11160 Belgrade, Serbia
e-mail: srdjan@aob.bg.ac.yu
e-mail: mcirkovic@aob.bg.ac.yu

Received 6 February 2008; accepted 12 June 2008

ABSTRACT

Context. Regarding the significant interest in both dark matter and the application of MOND to early-type galaxies, we investigate the MOND theory by comparing its predictions, for models of constant mass-to-light ratio, with observational data of the early-type galaxy NGC 4649.
Aims. We study whether measurements for NGC 3379 and NGC 1399 are typical of early-type systems and we test the assumption of a Newtonian constant M/L ratio underlying most of the published models.
Methods. We employ the globular clusters of NGC 4649 as a mass tracer. The Jeans equation is calculated for both MOND and constant mass-to-light ratio assumptions. Spherical symmetry is assumed and the calculations are performed for both isotropic and anisotropic cases.
Results. We found that both Jeans models with the assumption of a constant mass-to-light ratio and different MOND models provide good agreement with the observed values of the velocity dispersion. The most accurate fits of the velocity dispersion were obtained for the mass-to-light ratio in the *B*-band, which was equal to 7, implying that there is no need for significant amounts of dark matter in the outer parts (beyond 3 effective radii) of this galaxy. We also found that tangential anisotropies are most likely present in NGC 4649.

Key words. gravitation — galaxies: elliptical and lenticular, cD — galaxies: kinematics and dynamics — galaxies: haloes — galaxies:individual:NGC 4649

1. Introduction

The elliptical (early-type) galaxies are pressure-supported rather than rotationally supported systems and it is observationally more difficult to infer the presence of dark matter than in the more well-studied late-type galaxies. This is because, at large galactocentric distances, ellipticals do not have a straightforward tracer of circular orbits that is similar to the neutral hydrogen used to study the halo kinematics of spirals. Fortunately, however we are able to use several alternative tracers in the nearby ellipticals: 1) integrated stellar spectra (although the observations are limited practically within $\sim 3-4R_e$, where R_e is effective radius), 2) X-rays 3) planetary nebulae (PNe) and 4) globular clusters (GCs).

Studies of ellipticals have indicated that within $\sim 2-3R_e$ dark matter does not appear to dominate (e.g. Samurović & Danziger 2005, 2006). Beyond $\sim 3R_e$, dark matter appears to start to play important dynamical role. Although the presence of dark matter in the Universe is widely accepted, some alternative opinions have been expressed such as the theory of MOND (Milgrom 1983; recent reviews in Scarpa 2006, Milgrom 2008). The case for giant ellipticals has not been considered adequately and one possible reason is the scarcity of available kinematical data out to large galactocentric distances. Several attempts to model ellipticals with dark matter and/or MOND theory have appeared (e.g. Schuberth et al. 2006, Klypin & Prada 2007, Tiret et al. 2007, Richtler et al. 2008) with ambiguous results. Notably, Tiret et al. (2007) claimed that a MOND model for the dynamics of NGC 3379 reproduced the observations on all scales, while Richtler et al. (2008), studying NGC 1399, reached the opposite conclusion – that the best-fit MOND model still requires an "additional hypothetical dark halo". The latter result, for matter on small scales, agrees with observations implying the need for dark matter at the centers of clusters: for example, Angus, Famaey & Buote (2007) found that a hidden mass component (about 1.5 to 4 times more massive than the total visible mass) is required to explain the hydrostatic equilibrium of clusters with temperatures ranging from 0.7 to 8.9 keV.

In this paper, we discuss the early-type galaxy NGC 4649 (M60) belonging to the Virgo cluster, for which new observational data have become available (Lee et al. 2008a). This galaxy is more typical than either a field giant elliptical (NGC 3379) or the central galaxy of a cluster (NGC 1399), since it is a typical cluster member. The plan of the paper is as follows: in Sect. 2, we present the data related to NGC 4649; in Sect. 3, we calculate the total mass of this galaxy for Newtonian gravity and the MOND approach and solve the Jeans equation for the constant mass-to-light ratio and MOND approach to determine the best-fit parameters. Our conclusions are presented in Sect. 4.

2. Observational data

The data used in this paper are based on observations of GCs in NGC 4649 presented by Lee et al. (2008a). The sample consists of 121 GCs (83 blue and 38 red GCs). In all of our calculations, we always consider the entire sample, i.e. we do not divide the data into subsets, so that we are able to have a larger number of GCs per bin in our analyses.

NGC 4649 (M60) is a giant elliptical galaxy in the Virgo cluster that has a nearby companion, NGC 4647 (Sc galaxy at 2.′5 from the center of NGC 4649). The systemic velocity of NGC 4649 is $v_{\rm vel} = 1117 \pm 6$ km s^{-1}. We consider two values for the distance to NGC 4649: (i) the first one, $d = 17.30$ Mpc is based on the surface brightness fluctuation method and is taken from Lee et al. (2008a) (in this case, one arcsec corresponds to 84 pc); and (ii) the second one is based on the aforementioned systemic velocity, which implies that using the WMAP estimate of the Hubble constant from Komatsu et al. (2008) $h_0 = 0.70$, we obtain $d = 15.96$ Mpc, for which one arcsec corresponds to 77.5 pc. Both values of the distance are tested below and the most appropriate fit is presented. For the effective radius, we assume the value of $R_e = 90$ arcsec (equal to 7.56 kpc for $d = 17.30$ Mpc, and 6.97 kpc for $d = 15.96$ Mpc), which is the value taken from the paper by Kim et al. (2006). We note that there are different estimates in the literature, for example, Lee et al. (2008a) assumed $R_e = 110$ arcsec and according to the RC3 catalog (de Vaucouleurs et al. 1991), $R_e = 69$ arcsec. The discrepancy does not impact significantly our present conclusions.

We used the radial velocities of GCs to determine the kinematics of NGC 4649: we calculated the velocity dispersion, the skewness and kurtosis parameters, s_3 and s_4, using standard definitions and the NAG routine `G01AAF`. We note that our intention is not to reconstruct the full line-of-sight velocity distribution, because it is known (see Merritt 1997) that for small data sets such as the one we consider here, that contain less than a few hundred objects per bin, this is impossible. We note, however, that Wu & Tremaine (2006) developed a maximum likelihood method for determination the mass distribution in spherical stellar systems that uses test particles and applied this method successfully to a giant elliptical M87 using 161 GCs found in this galaxy.

We therefore calculate skewness and kurtosis parameters to determine whether, in some bins, a significant departure from a Gaussian distribution (and a tendency toward some particular type of orbits) exists. This is similar to the approach applied by Teodorescu et al. (2005) in their Fig. 18. Our results regarding departures from a Gaussian distribution are applied below where we apply different anisotropies when solving the Jeans equation. The results are given in Fig. 1 and in Table 1. What is obvious from the data (and what makes this galaxy a good candidate for the dynamical modeling based on two different techniques) is that the velocity dispersion appears to be constant throughout the entire galaxy, and, based on the values of s_4 (small negative values but consistent with zero), there appears to be a tendency towards tangential orbits; the same conclusion based on Jeans modeling was reached by Hwang et al. (2008) (and also by Bridges et al. (2006), who found that the orbital distribution beyond 100 arcsec becomes tangentially biased).

For the Jeans modeling presented below, we also needed to determine the radial surface density profile of the clusters in NGC 4649. This plot is given in Fig. 2 and represents the radial distribution of the total sample of GCs in NGC 4649 as a function of radius. The fit is given by a power law of the form: $\Sigma \propto r^{-\gamma}$. Using the least squares method, we decided that, within a galactocentric radius of approximately 1 arcmin $\gamma = 0.338$, and for the region beyond 1 arcmin, that we should use the value $\gamma = 1.285$ derived by Lee et al. (2008b).

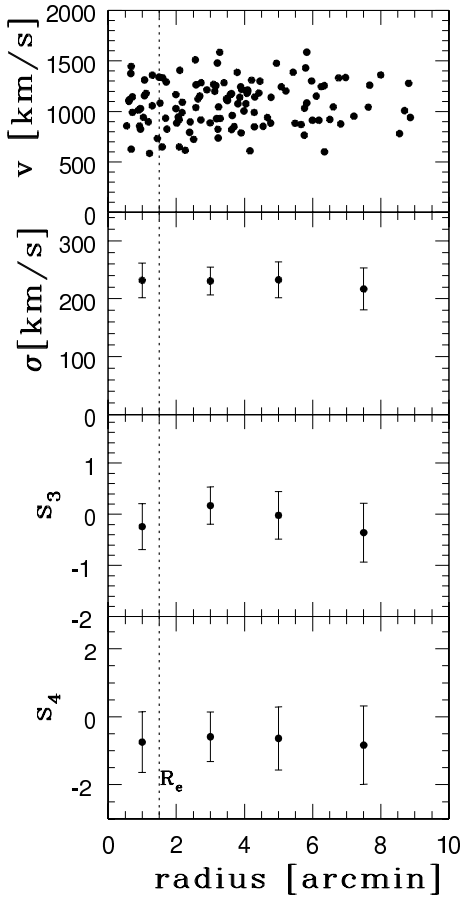

Fig. 1. Kinematics of NGC 4649 based on the total sample of red and blue GCs. From top to bottom: radial velocity of the GCs in km s^{-1}; velocity dispersion calculated in a given bin; and the s_3 and s_4 parameters, which describe symmetric and asymmetric departures from the Gaussian, respectively.

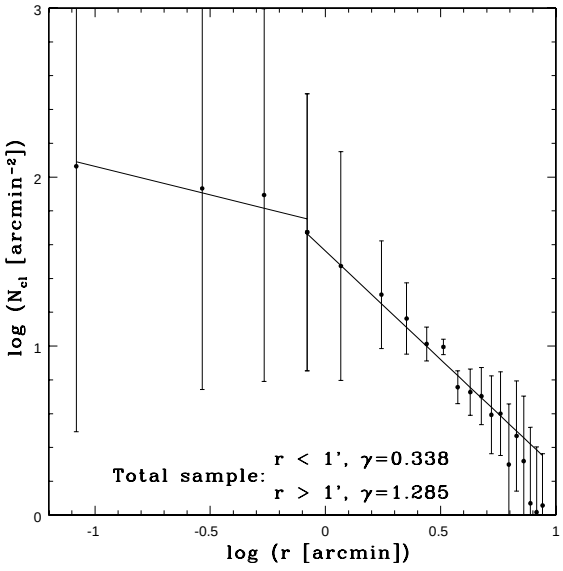

Fig. 2. Radial distribution of GCs (both blue and red) in NGC 4649. A power law is fitted to the radial surface density of GCs: $\Sigma \propto r^{-\gamma}$ (see text for details).

Table 1. Kinematics data for NGC 4649 for the total sample of clusters

$< r >$ (arcmin) (1)	$\sigma_{\rm total}$ (km s^{-1}) (2)	err_$\sigma_{\rm total}$ (km s^{-1}) (3)	$s_{3\rm total}$ (4)	err_$s_{3\rm total}$ (5)	$s_{4\rm total}$ (6)	err_$s_{4\rm total}$ (7)	N (8)
1	232	30	-0.03	0.06	-0.04	0.04	30
3	231	24	0.02	0.05	-0.03	0.04	45
5	233	31	0.00	0.07	-0.03	0.05	28
7.5	217	36	-0.05	0.08	-0.04	0.06	18

NOTES – Col. (1): central point for a given bin. Col. (2): velocity dispersion for the total sample of clusters. Col. (3): formal errors for the velocity dispersion of the total sample of clusters. Col. (4): s_3 parameter for the total sample of clusters. Col. (5): formal errors for the s_3 parameter for the total sample of clusters. Col. (6): s_4 parameter for the total sample of clusters. Col. (7): formal errors for the s_4 parameter for the total sample of clusters. Col. (8): number of clusters in a given bin.

3. Models

We model the observed velocity dispersion beyond 1 arcmin (because our observationally based points are all beyond $\sim$ 1 arcmin) using the Jeans equation (e.g. Binney & Tremaine 1987):

$$\frac{{\rm d}\sigma_r^2}{{\rm d}r} + \sigma_r^2 \frac{(2\beta_* + \alpha)}{r} = -\frac{GM(r)}{r^2} + \frac{v_{\rm rot}^2}{r} \quad (1)$$

where σ_r is the radial stellar velocity dispersion, $\alpha = {\rm d}\ln\rho/{\rm d}\ln r$ is the slope of tracer density ρ (the surface density is given above and in the models below we use $\alpha = -2.285$). The rotation speed $v_{\rm rot}$ was found to be non-zero, i.e. $v_{\rm rot} = 141^{+50}_{-38}$ km s^{-1} (Hwang et al. 2008) and is used in all modeling below. A parameter β_* is introduced to describe the non-spherical nature of the stellar velocity dispersion:

$$\beta_* = 1 - \frac{\overline{v_\theta^2}}{\sigma_r^2}, \quad (2)$$

where $\overline{v_\theta^2} = \overline{v_\theta}^2 + \sigma_\theta^2$. For $0 < \beta_* < 1$, the orbits are predominantly radial, and the line-of-sight velocity distribution is more strongly peaked than a Gaussian profile (positive s_4 parameter), and for $-\infty \leq \beta_* < 0$ the orbits are mostly tangential, so that the profile is more flat–topped than a Gaussian (negative s_4 parameter) (Gerhard 1993).

In all models below, we calculated the projected line-of-sight velocity dispersion (e.g. Binney & Mamon 1982; Mathews & Brighenti 2003):

$$\sigma_p^2(R) = \frac{\int_R^{r_t} \sigma_r^2(r)\left[1 - (R/r)^2\beta_*\right]\rho(r)(r^2 - R^2)^{-1/2} r{\rm d}r}{\int_R^{r_t} \rho(r)(r^2 - R^2)^{-1/2} r{\rm d}r} \quad (3)$$

where the truncation radius, r_t, extends beyond the observed kinematical point of highest galactocentric radius. We assumed in all the cases that $r_t \sim 7R_e$.

3.1. Newtonian mass-follows-light models

A relation for determining the typical mass-to-light ratio in elliptical galaxies was given by van der Marel (1991), who found for 37 bright ellipticals that the average mass-to-light ratio in the B–band in solar units was: $M/L_B = (5.93 \pm 0.25)\, h_{50}$ becoming $M/L_B = (11.86 \pm 0.50)\, h$ and therefore $M/L_B = 8.30 \pm 0.35$ for $h = 0.7$. Since this study addressed the inner parts of ellipticals, we considered the absolute upper limit for the *visible (stellar)* component to be $M/L_B \sim 9 - 10$. An inferred mass-to-light ratio of over approximately 10 in a given region would therefore imply the existence of dark matter.

For constant mass-to-light ratio models, we consider relations that include stellar mass and dark matter distributed in the form of the standard Hernquist (1990) profile:

$$\rho_H(r) = \frac{M_T}{2\pi}\frac{a}{r}\frac{1}{(r+a)^3}, \quad (4)$$

which has two parameters: the total mass M_T and scale length, a, where $R_e = 1.8153a$. We solve the Jeans equation (Eq. 1) and consider values of M/L_B of between 7 and 15, while repeating that $M/L_B \gtrsim 10$ is incompatible with an entirely stellar component. As can be seen from Fig. 3, we tested 3 values of the mass-to-light ratio that are presented by the hatched stripes: low ($M/L_B = 7$), intermediate ($M/L_B = 10$), and high ($M/L_B = 15$, includes at least $\sim$ 50% of dark matter). In all cases, we allowed a realistic variation in both the β_* parameter and the distance to the galaxy, d for the fixed value of the mass-to-light ratio. If we need to identify the constant mass-to-light ratio that most accurately describes the observed velocity dispersion data, we would present the model with the following parameters: lower mass-to-light ratio, $M/L_B = 7$, slightly tangential orbits, $\beta_* = -0.2$, and the distance $d = 17.30$ Mpc (see Fig. 3 and Table 2). We note that a good fit can also be achieved for a higher value of the mass-to-light ratio but then the β_* parameter rises and the orbits become isotropic (see Fig. 3, central "S2" stripe, which presents a case for which $M/L_B = 10$).

With the assumption of the constant mass-to-light ratio the overall conclusion of the Jeans modeling is that, although we detect a hint of a rising mass-to-light ratio with increasing radius, due to the large error bars, we can obtain a satisfactory fit by also assuming a constant value $M/L_B \sim 7$, which implies that dark matter is not playing an important dynamical role, even beyond $\sim 3R_e$. The value of the constant mass-to-light ratio $M/L_B \sim 7$ implies that the total mass of NGC 4649 is equal to $\sim 5\times10^{11} M_\odot$ at $\sim 3R_e$. This estimate is in agreement with predictions based on the assumption that the Virial theorem holds (see Bertin et al. 2002; Cappellari et al. 2006). This total mass is used below.

3.2. MOND models

We follow the recommendation of our referee and calculate the total mass of NGC 4649 in MOND gravity using three different formulas: (i) the "simple" MOND formula from Famaey & Binney (2005), (ii) the "standard" formula (Sanders & McGaugh 2002), and (iii) the Bekenstein's "toy" model (Bekenstein 2004). We write the Newtonian acceleration as $a_N = a\mu(a/a_0)$, where a is the MOND acceleration, $\mu(x)$ is the MOND interpolating function where $x \equiv a/a_0$, and $a_0 = 1.35^{+0.28}_{-0.42} \times 10^{-8}$ cm s^{-2} is a

universal constant (Famaey et al. 2007). The interpolation function $\mu(a/a_0)$ shows an asymptotic behavior, $\mu \approx 1$, for $a \gg a_0$, and we derive the Newtonian relation in the strong field regime, and $\mu = a/a_0$ for $a \ll a_0$. The MOND dynamical mass, M_M, can be expressed in terms of the Newtonian values, M_N using the following expression (e.g. Angus et al. 2007):

$$M_M(r) = M_N(r) \times \mu(x). \tag{5}$$

The intepolation function can have different forms as given below.

1. A "simple" MOND formula is given by:

$$\mu(x) = \frac{x}{1+x}. \tag{6}$$

In this case, the circular velocity curve can be written as (e.g. Richtler et al. 2008)

$$V^2_{\rm circ,M} = \frac{V^2_{\rm circ,N}}{2} + \sqrt{\frac{V^4_{\rm circ,N}}{4} + V^2_{\rm circ,N} \times a_0 \times r}, \tag{7}$$

where $V_{\rm circ,N}$ is the Newtonian circular velocity.

2. A "standard" MOND formula is given by:

$$\mu(x) = \frac{x}{\sqrt{1+x^2}}. \tag{8}$$

It can be shown that the circular velocity curve then becomes:

$$V^4_{\rm circ,M} = \frac{V^4_{\rm circ,N}}{2} + \sqrt{\frac{V^8_{\rm circ,N}}{4} + V^4_{\rm circ,N} \times a_0^2 \times r^2}. \tag{9}$$

3. Finally, for the "toy" model the MOND formula is:

$$\mu(x) = \frac{-1+\sqrt{1+4x}}{1+\sqrt{1+4x}}. \tag{10}$$

After some arithmetic, we derive the expression for the circular velocity curve:

$$V^2_{\rm circ,M} = V^2_{\rm circ,N} + \sqrt{a_0 \times r}\, V_{\rm circ,N}. \tag{11}$$

These three MOND models are tested below using Jeans models, and the best-fit model parameters are indicated in each case.

We solved the Jeans equation (Eq. 1) based on the Hernquist profile (Eq. 4), where M_T is calculated using Eq. 5. We varied different parameters: distance d, parameter a_0, and anisotropy β_*. The best-fit models are presented in Fig. 4 and Table 2. We tested all three MOND models and it can be seen that the best fits were obtained for higher value of the distance, $d = 17.30$ Mpc. We note that the quality of the fits for all MOND models was approximately the same, as in the case of the constant mass-to-light ratio models, as indicatated by the reduced χ^2 values (see column 6 in Table 2). We formed our Jeans models based on an expression for the mass corresponding to each of the constant mass-to-light ratios, as in the previous section. The lower mass-to-light ratio ($M/L_B = 7$) provides a good fit to the observed velocity dispersion for all tested models. The preferred value of the constant $a_0 = 1.35 \times 10^{-8}$ cm s^{-1} was found in two cases (for the "simple" and "toy" model), whereas a lower value was found for the "standard" model, $a_0 = 0.93 \times 10^{-8}$ cm s^{-1}. In all tested models, we found that there is a detection of tangential anisotropy, the largest extent for the "toy" model ($\beta_* = -0.5$) and the smallest extent for the "standard" model ($\beta_* = -0.3$). It is important to emphasize that we cannot exclude higher (but not extremely high, see below) mass-to-light ratio in our models; for example, the "toy" model with $M/L_B = 9$, $a_0 = 0.93 \times 10^{-8}$ cm s^{-1}, $d = 17.30$ Mpc, and ($\beta_* = -0.3$) also provides a satisfactory fit to the observed data with reduced $\chi^2 = 2.90$. In general, because of the large observational error bars at this stage, we cannot exclude the possibility of an increase in the velocity dispersion in the outer parts, which would imply the increase of the total mass-to-light ratio and the existence of dark matter. We emphasize that these models are based on a constant mass-to-light ratio and, therefore, a fixed higher value of the mass-to-light ratio, in principle corresponds to a higher velocity dispersion close to the center and a more realistic value in the outer parts of NGC 4649.

It is known that the "external field effect" is a phenomenological requirement of MOND, which has strong implications for non-isolated systems (Sanders & McGaugh 2002), such as NGC 4649. This effect is complicated and was analyzed in detail by Wu et al. (2007); here, we provide only an approximate estimate of this effect on our results. We follow Famaey et al. (2007b) and calculate the gravitational force per unit mass exerted by the Virgo cluster on NGC 4649:

$$a_{\rm ext} = \frac{(GM^b_{\rm Vir}a_0)^{1/2}}{d_c} \simeq 0.15 a_0 \tag{12}$$

where $M^b_{\rm Vir} = 2.1 \times 10^{13} M_\odot$ is the baryonic mass of the Virgo inside $d_c \sim 1$ Mpc (which is the distance of NGC 4649 from the center of the Virgo cluster; the distance to NGC 4649 is equal to 17.30 Mpc and is also used) taken from the paper by McLaughlin (1999) (his figure 2) who estimated that a global baryon fraction in Virgo is $\sim$ 7%. We then apply the external effect by inserting $\mu(|\mathbf{a} + \mathbf{a}_{\rm ext}|/a_0)$ only in the case of the "toy" model to infer the effects on the Jeans modeling. The result is plotted in Fig. 4 with the dotted line (and is also given in Table 2). The modeled velocity dispersion is higher than in the case when we neglect the external field but not by much. This result is again consistent with a hypothesis of no dark matter. Parenthetically, the same reasoning applies much more forcefully to the acceleration due to the presence of the galaxy companion NGC 4647, for which the value in Eq. 12 is smaller for between one and two orders of magnitude, depending on the baryonic mass estimate for the companion.

The same conclusion regarding the dynamical importance of dark matter reached in the case of the constant mass-to-light ratio also holds for the Jeans models based on MOND: successful fits were obtained without dark matter throughout the entire galaxy for all MOND approaches.

4. Conclusions

The GCs kinematics of NGC 4649 was studied out to 260 arcsec (= $2.9R_e$ using the value of effective radius adopted in this paper) by Bridges et al. (2006). They found, using isotropic and axisymmetric orbit-based models, that dark matter exists in the halo of this galaxy.

In this paper, we have studied the dynamics of the early-type galaxy NGC 4649 (M60) for both Newtonian and MOND approaches using the Jeans equation and found that there is no need for significant amount of dark matter in its outer parts. The principle results of our study were:

1. We studied the kinematics of NGC 4649 and found that the velocity dispersion remains approximately constant through-

Table 2. Best fits for constant M/L ratio and MOND modeling

Model (1)	M/L_B (2)	a_0 [10^{-8} cm s^{-2}] (3)	d [Mpc] (4)	β_* (5)	χ^2 (6)
Const	7	—	17.30	-0.2	1.36
MOND Simple	7	1.35	17.30	-0.4	2.31
MOND Standard	7	0.93	17.30	-0.3	1.66
MOND Toy	7	1.35	17.30	-0.5	1.83
MOND Toy (ext. field)	7	1.35	17.30	-0.5	1.78

NOTES – Col. (1): the name of the model; "ext. field" is for the MOND toy model for which the external field was taken into account (see text for details). Col. (2): mass-to-light ratio in the *B*-band used. Col. (3): the best-fit function value of the constant a_0; it is not used in the case of the model with the constant mass-to-light ratio. Col. (4): the best fitting value of distance to NGC 4649. Col. (5): the best fitting value of the β_* parameter. Col. (6): reduced χ^2 of the best fit for a given model.

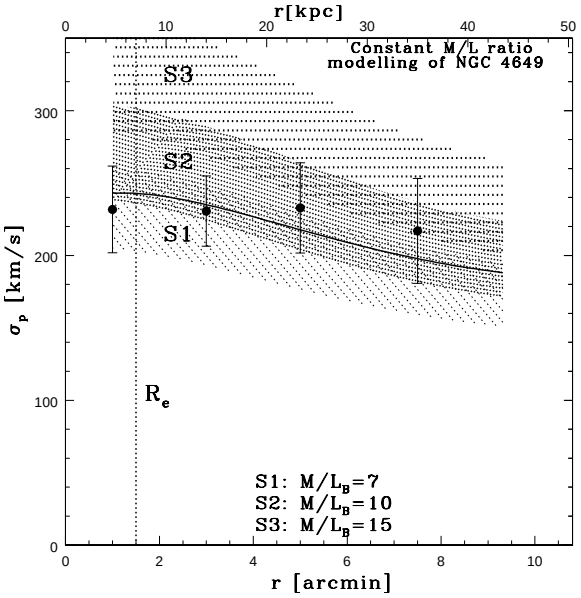

Fig. 3. Jeans modeling of NGC 4649 using the constant M/L approach. Three different stripes, which correspond to three different constant mass-to-light ratios, are given and the upper limit is always determined for $\beta_* = -0.2$, and $d = 15.96$ Mpc while the lower limit is determined for $\beta_* = 0.2$ and $d = 17.30$ Mpc. The lowest stripe "S1" is for the constant mass-to-light ratio $M/L_B = 7$, the stripe in between, "S2" is for $M/L_B = 10$, and the upper stripe, "S3" is for $M/L_B = 15$. The solid line is the best fit obtained for the constant mass-to-light ratio models: in this case $M/L_B = 7$, $\beta_* = -0.2$ and $d = 17.30$ Mpc. The upper scale corresponds to the distance $d = 17.30$ Mpc.

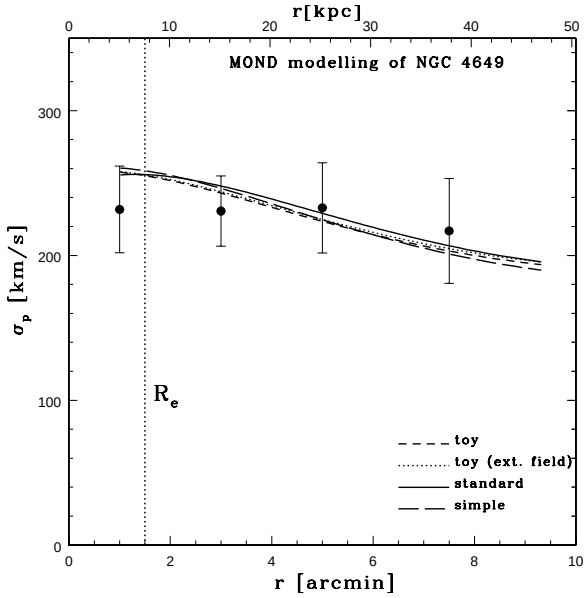

Fig. 4. Jeans modeling of NGC 4649 using the MOND approach and $M/L_B = 7$. Solid line is for the "standard" model for which $a_0 = 0.93 \times 10^{-8}$ cm s^{-2} and $\beta_* = -0.3$. Long-dashed line is for the "simple" model for which $a_0 = 1.35 \times 10^{-8}$ cm s^{-2} and $\beta_* = -0.4$. For the "toy" model we present two fits for which $a_0 = 1.35 \times 10^{-8}$ cm s^{-2} and $\beta_* = -0.5$: (i) short-dashed line for the case when the external field is absent (ii) dotted line for the case when the external field is present. In this figure the upper scale corresponds to $d = 17.30$ Mpc because the best fits in all the cases were obtained using this distance.

out the entire galaxy. We detected an observational hint of small tangential anisotropies in this galaxy, which agrees with other results in the literature (Bridges et al. 2006, Hwang et al. 2008).

2. We used the Jeans equation to infer the mass-to-light ratios that can describe the observed velocity dispersion profile of NGC 4649: we found that the successful fit to the velocity dispersion can be obtained using $M/L_B \sim 7$ with moderate tangential anisotropies that indicate the lack of dark matter throughout this galaxy. Higher values of the mass-to-light ratios ($M/L_B \sim 9 - 10$), which are still consistent with a no dark matter hypothesis, are also permitted but then the anisotropies tend to vanish.
3. We also used the Jeans equation to test the predictions of the MOND theory using three different models: "simple", "standard", and "toy". We found that all the tested MOND models provided a good fit to the observational velocity dispersion data (again for $M/L_B \sim 7$ with moderate tangential anisotropies).
4. We have also briefly addressed the problem of the surrounding environment, since NGC 4649 belongs to the Virgo cluster. We found that the external field at the position of NGC 4649 does not significantly alter our conclusions: the Bekenstein "toy" model again provides a good fit to the observed velocity dispersion (assuming $M/L_B \sim 7$) and is consistent with a no dark matter hypothesis.

Acknowledgements. We thank H. S. Hwang for providing us the data in electronic form. This work was supported by the Ministry of Science of the

Republic of Serbia through the project no. 146012, “Gaseous and stellar component of galaxies: interaction and evolution”. This research has made use of the NASA/IPAC Extragalactic Database (NED) which is operated by the Jet Propulsion Laboratory, California Institute of Technology, under contract with the National Aeronautics and Space Administration. We acknowledge the usage of the HyperLeda database (http://leda.univ-lyon1.fr). We thank the anonymous referee for the very useful and detailed comments which helped to significantly improve the quality of the manuscript.

References

Angus, G.W., Famaey, B. & Buote, D.A., 2008, MNRAS, 387, 1470
Bekenstein, J., 2004, Phys. Rev. D, 70, 083509
Bertin, G., Ciotti, L. & Del Principe, M.: 2002, A&A, 386, 149
Binney, J.J. & Mamon, G., 1982, MNRAS, 200, 361
Binney, J.J. & Tremaine, S., 1987, Galactic Dynamics, (Princeton Univ. Press, Princeton)
Bridges, T., Gebhardt, K., Sharples, R. et al., 2006, MNRAS, 373, 157
Cappellari, M., Bacon, R, Bureau, M. et al.: 2006, MNRAS, 360, 1126
de Vaucouleurs, G., de Vaucouleurs, A. Corwin, H.G. Jr., et al., 1991, Third Reference Catalogue of Bright Galaxies, (Springer-Verlag, New York)
Famaey, B. & Binney, J., 2005, MNRAS, 363, 603
Famaey, B., Gentile, G., Bruneton, J.-P. & Zhao, H.S., 2007a, Phys. Rev. D, 75
Famaey, B., Bruneton, J.-P. & Zhao, H.S, 2007b, MNRAS, 377, L79
Gerhard, O., 1993, MNRAS, 265, 213
Hernquist, L. 1990, ApJ, 356, 359
Hwang, H.S, Lee, M.G., Park, H.S., et al., 2008, ApJ, 674, 869
Kim, E., Kim, D.–W., Fabbiano, G., et al., 2006, ApJ, 647, 276
Komatsu, E., Dunkley, J., Nolta, M.R., et al., 2008, ApJSS, submitted [arXiv: astro-ph/0803.0547]
Klypin, A., & Prada, F., 2007 [arXiv:astro-ph/0706.3554]
Lee, M.G., Hwang, H.S, Park, H.S., et al., 2008a, ApJ, 674, 857
Lee, M.G., Park, H.S., Kim, E., Hwang, H.S, Kim, S.C. & Geisler, D., 2008b, ApJ, 682, 135
Mathews W.G. & Brighenti F., 2003, ApJ, 599, 992
McLaughlin, D.E., 1999, ApJ, 512, L9
Merritt, D., 1997, AJ, 114, 228
Milgrom, M., 1983, ApJ, 270, 365
Milgrom, M., 2008, [arXiv: astro-ph/0801.3133]
Richtler, T, Schuberth, Y., Hilker, M., Dirsch, B., Bassino, L. and Romanowsky, A.J. 2008, A&A, 478, L23
Samurović, S. & Danziger, I.J., 2005, MNRAS, 363, 769
Samurović, S. & Danziger, I.J., 2006, A&A, 458, 79
Sanders, R.H. & McGaugh, S., 2002, ARA&A, 40, 263
Scarpa, R., 2006, in “The First Crisis in Cosmology”, Eds., E.J. Lerner & J.B. Almeida (AIP Conference Proceedings, Vol. 822), 253
Schuberth, Y., Richtler, T., Dirsch, B. et al., 2006, A&A, 459, 391
Teodorescu A.M., Méndez R.H., Saglia R.P. et al., 2005, ApJ, 635, 290
Tiret, O., Combes, F., Angus, G.W., Famaey, B. & Zhao, H.S., 2007, A&A, 476, L1
van der Marel R. P., 1991, MNRAS, 253, 710
Wu, X. & Tremaine, S., 2006, ApJ, 643, 210
Wu, X., Zhao, H.S. & Famaey, B., 2007, ApJ, 665, L101